

**Electronic Supporting Information**

**Effects of Intramolecular Hydrogen Bonding on the Conformation and Luminescence Property of Dibenzoylpyridine-based Thermally Activated Delayed Fluorescence Materials**

Jayabalan Pandidurai, Jayachandran Jayakumar, Natarajan Senthilkumar, and Chien-Hong Cheng<sup>\*a</sup>

<sup>a</sup>Departments of Chemistry, National Tsing Hua University, Hsinchu 30013, Taiwan.

E-mail: [chcheng@mx.nthu.edu.tw](mailto:chcheng@mx.nthu.edu.tw)

<b>Table of Contents</b>	<b>Page No</b>
General Information	S-2
Experimental section	S-2
TD-DFT for singlet ( $S_1$ ) and triplet ( $T_1$ ) states	S-3
Photophysical properties	S-6
Transient PL and thermal properties	S-7
Electrochemical properties and chemical structures of the device materials	S-8
EL-properties of the devices	S-9
References	S-11
Spectral data of compounds	S-12
ORTEP Diagram and X-ray data of emitters	S-15
Mass spectral analysis of TADF emitters	S-20

## **General Information**

<sup>1</sup>H NMR and <sup>13</sup>C NMR spectra were measured on a Mercury 400 spectrometer. UV-vis absorption spectra were recorded on a U-3310 recording spectrophotometer. PL spectra were recorded on an F-7000 fluorescence spectrophotometer. The differential scanning calorimetry (DSC) was performed on a DSC Q10 unit at a heating rate of 10 °C/min. from 50 °C to 300 °C under argon. The glass transition temperature ( $T_g$ ) was determined from the second heating scan. Transient PL decay measurements were done using an Edinburgh FLS 980 instrument. Cyclic voltammetry (CV) was measured with a CHI-600 voltammetric analyzer. Tetrabutyl ammonium perchlorate (TBAClO<sub>4</sub>) (0.1 M) was used as a supporting electrolyte. The conventional three-electrode configuration consists of a platinum working electrode, a platinum wire auxiliary electrode, and an Ag wire pseudo-reference electrode with ferrocenium-ferrocene (Fc+/Fc) as the internal standard.

## **DFT Calculation**

Molecular geometry optimizations and electronic properties of these materials were carried out by using the Gaussian 09 program with density functional theory (DFT) and time-dependent DFT (TD-DFT for S<sub>1</sub> and T<sub>1</sub> states) calculations in which the Becke's three-parameter functional combined with Lee, Yang, and Parr's correlation functional (B3LYP) hybrid exchange-correlation functional with the 6-31G\* basis set was used.<sup>1</sup> The molecular orbitals were visualized by Gaussview 5.0 software.<sup>1,2</sup> All calculations were performed in the gas phase.

## **OLEDs Fabrication and Measurement**

Organic materials used in device fabrication were purified by sublimation. Devices were fabricated by vacuum deposition onto pre-coated ITO glass with a sheet resistance of 15 Ω/square at a pressure lower than 10<sup>-6</sup> Torr. Organic materials were deposited at the rate of 0.5~1.2 Å s<sup>-1</sup>. LiF and Al were deposited at the rate of 0.1 Å s<sup>-1</sup>, 3-10 Å s<sup>-1</sup>, respectively. The rest of the procedures is similar to the reported method.<sup>2</sup> Current-voltage-luminance (I-V-L) characterization and electroluminescent spectra were measured and recorded by using a programmable source meter (2400, Keithley) and a spectroradiometer (CS2000A, Konica Minolta). External quantum efficiencies and power efficiencies were determined by the Lambertian emission device assumption.

## **Synthesis of TADF compounds.**

The compounds 10-(4-bromophenyl)-9,9-dimethyl-9,10-dihydroacridine,<sup>3</sup> 10-(4-bromophenyl)-10H-phenoxyazine<sup>4</sup> and 2-cyanopyridine-5-carboxaldehyde<sup>3</sup> were prepared according to the procedure known in the literature.

**Table S1.** Singlet and triplet excitation states, and transition configurations of the 26DAcBPy by TD-DFT at the B3LYP/6-31G (d,p).

State	Excitation		$E_{\text{cal}}$ (eV) <sup>a</sup>	$\lambda_{\text{cal}}$ (nm) <sup>b</sup>	$f^{\text{c}}$
Singlet Excited States					
S1	HOMO-1 → LUMO+1	0.19433	2.0059	618	0.0000
	HOMO → LUMO	0.67571			
S2	HOMO-1 → LUMO	0.66567	2.0220	650	0.0000
	HOMO → LUMO+1	0.22563			
S3	HOMO-1 → LUMO	-0.23066	2.2484	551	0.0001
	HOMO → LUMO+1	0.66696			
S4	HOMO-1 → LUMO+1	0.67671	2.0608	547	0.0003
	HOMO → LUMO	-0.19944			
Triplet Excited States					
T1	HOMO-1 → LUMO+1	0.19920	2.0021	619	-
	HOMO → LUMO	0.67377			
T2	HOMO-1 → LUMO	0.66316	2.0180	614	-
	HOMO → LUMO+1	0.23129			
T3	HOMO-1 → LUMO	-0.23709	2.2467	551	-
	HOMO → LUMO+1	0.66427			
T4	HOMO-1 → LUMO+1	0.39208	2.2632	547	-
	HOMO → LUMO+1	-0.20496			
$S1-T1 = \Delta E_{\text{ST}}$ $2.0059 - 2.0021 = 0.0038 \text{ eV}$ H-bonding distance = 2.4 Å					

<sup>a</sup>Excitation energy, <sup>b</sup>excitation wavelength ( $\lambda$ ), <sup>c</sup>oscillator strength ( $f$ ).

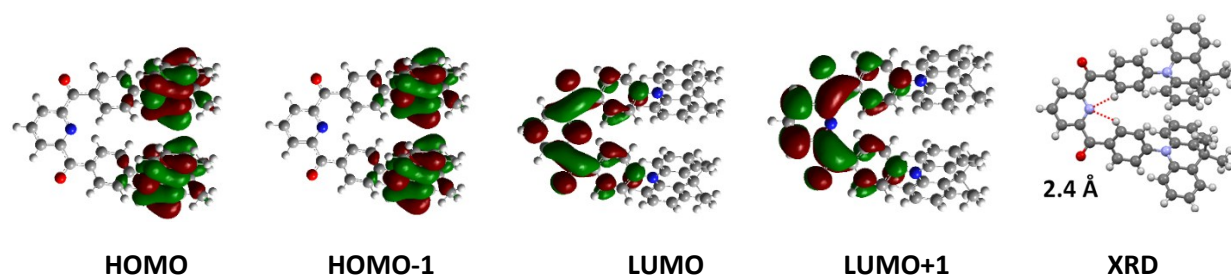


**Table S2.** Singlet and triplet excitation states, and transition configurations of the 25DAcBPy by TD-DFT at the B3LYP/6-31G (d,p).

State	Excitation		$E_{\text{cal}}$ (eV) <sup>a</sup>	$\lambda_{\text{cal}}$ (nm) <sup>b</sup>	$f^{\text{c}}$
Singlet Excited States					
S1	HOMO → LUMO HOMO → LUMO+1	0.69285 -0.13385	2.1946	564	0.0012
S2	HOMO-1 → LUMO	0.70496	2.6439	468	0.2407
S3	HOMO → LUMO HOMO → LUMO+1	0.13861 0.68248	2.9686	417	0.0013
S4	HOMO-3 → LUMO HOMO-3 → LUMO+1	0.65684 0.21079	3.0927	400	0.0032
Triplet Excited States					
T1	HOMO → LUMO HOMO → LUMO+1	0.69085 -0.13950	2.1879	566	-
T2	HOMO-1 → LUMO HOMO → LUMO+1	0.63180 0.24193	2.2228	557	-
$S1-T1 = \Delta E_{\text{ST}} \quad 2.1946 - 2.1879 = 0.0067 \text{ eV} \quad \text{H-bonding distance} = 2.3 \text{ \AA}$					

<sup>a</sup>Excitation energy, <sup>b</sup>excitation wavelength ( $\lambda$ ), <sup>c</sup>oscillator strength ( $f$ ).

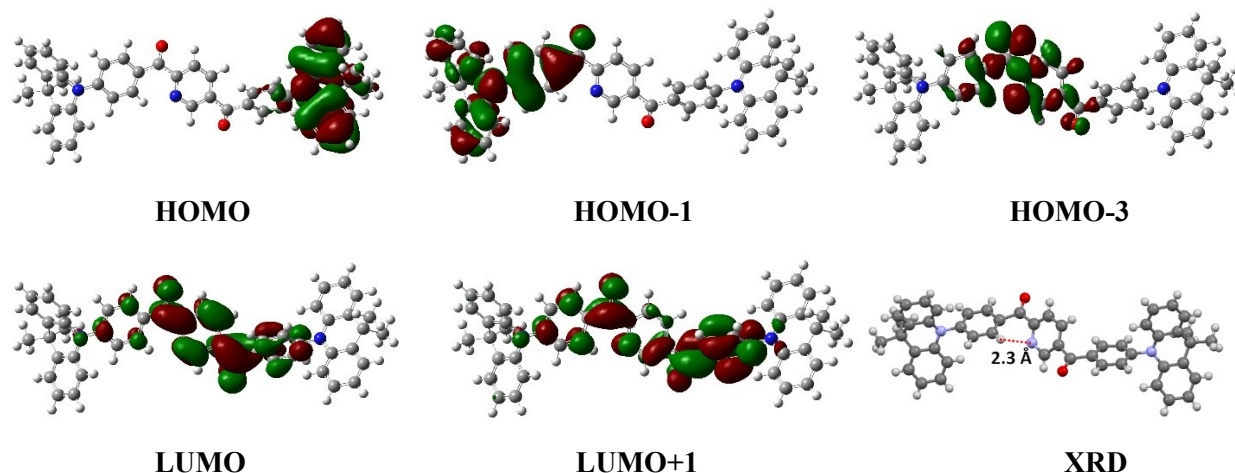
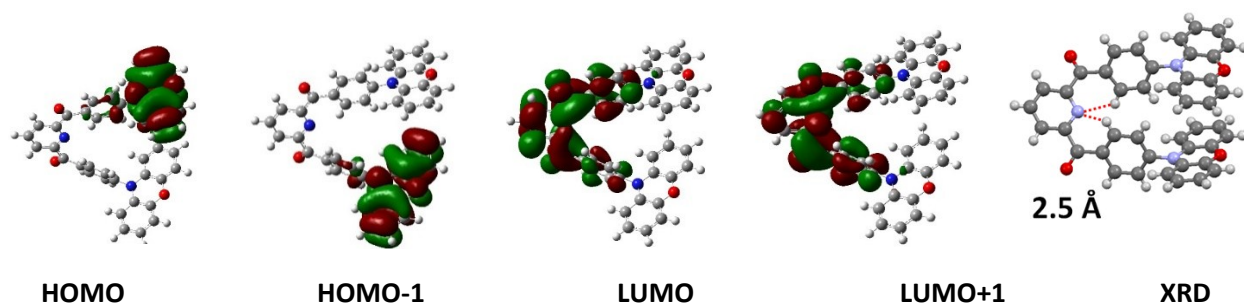


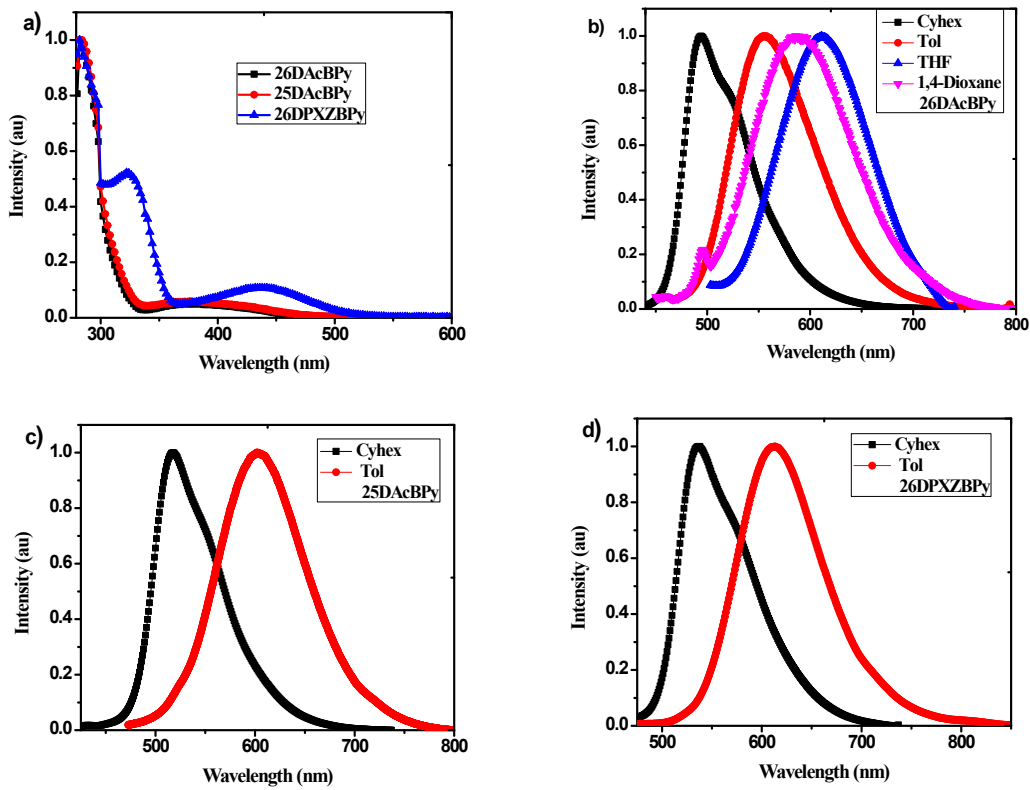
**Table S3.** Singlet and triplet excitation states, and transition configurations of the 26DPXZBPy by TD-DFT at the B3LYP/6-31G(d,p).

State	Excitation		$E_{\text{cal}}$ (eV) <sup>a</sup>	$\lambda_{\text{cal}}$ (nm) <sup>b</sup>	$f^c$
Singlet Excited States					
S1	HOMO → LUMO	0.67150	1.8018	688	0.0290
	HOMO → LUMO+1	0.20423			
S2	HOMO-1 → LUMO	0.61729	1.9062	650	0.0169
	HOMO-1 → LUMO+1	-0.33283			
S3	HOMO → LUMO	-0.20722	2.0258	612	0.016
	HOMO → LUMO+1	0.61872			
S4	HOMO-1 → LUMO	0.33869	2.0608	601	0.118
	HOMO-1 → LUMO+1	0.61872			
Triplet Excited States					
T1	HOMO → LUMO	0.65468	1.7377	713	-
	HOMO → LUMO+1	0.24530			
T2	HOMO-1 → LUMO	0.58512	1.8694	663	-
	HOMO-1 → LUMO+1	-0.38301			
T3	HOMO → LUMO	-0.25225	2.0206	613	-
	HOMO → LUMO+1	0.65944			
T4	HOMO-1 → LUMO	0.39208	2.0540	603	-
	HOMO-1 → LUMO+1	0.5862			
$S1-T1 = \Delta E_{\text{ST}} \quad 1.8018 - 1.7377 = 0.0641 \text{ eV} \quad \text{H-bonding distance} = 2.5 \text{ \AA}$					

<sup>a</sup>Excitation energy, <sup>b</sup>excitation wavelength ( $\lambda$ ), <sup>c</sup>oscillator strength ( $f$ ).

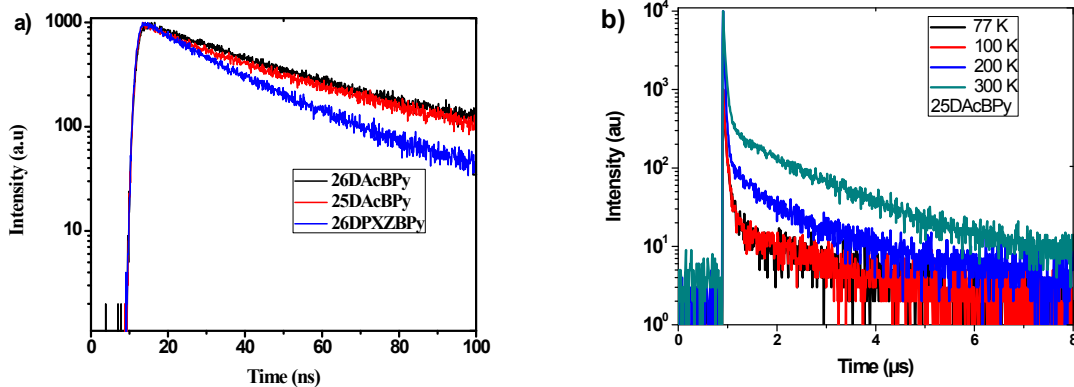


## Photophysical properties



**Fig. S1.** a) UV-Vis spectra of 26DAcBPY, 25DAcBPY and 26DPXZBPY in toluene solution at RT ( $10^{-5}$  M); and b) PL spectra of 26DAcBPY, c) 25DAcBPY and d) 26DPXZBPY in various solvents at RT ( $10^{-5}$  M).

## Transient PL and thermal properties



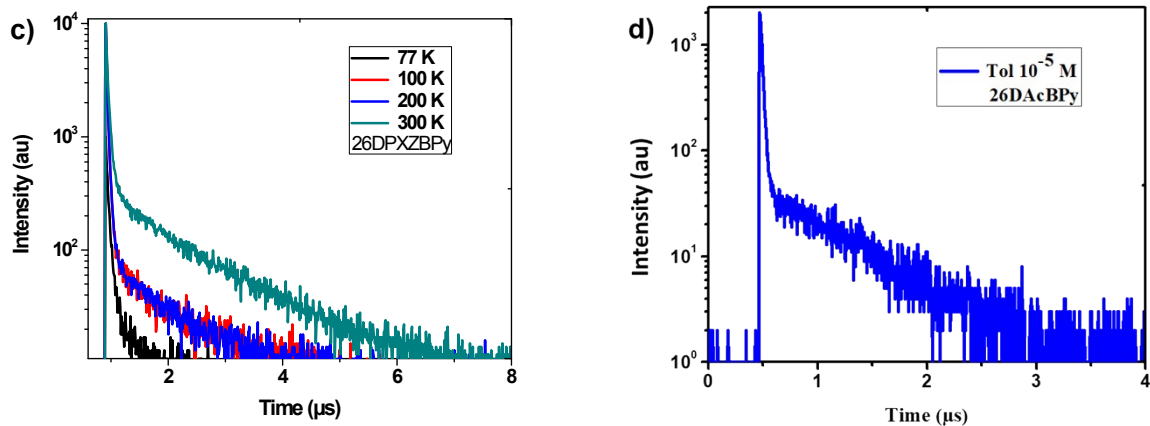


**Fig. S2:** a) Prompt decay curves of emitters in the thin film (10 wt% doped in mCBP) at 300 K. b) The temperature-dependent transient PL decay for 25DAcBPY and c) 26DPXZBPY measured in the thin film (10 wt% doped in mCBP) at various temperatures. (d) PL decay curve of 26DAcBPY measured in toluene ( $10^{-5}$  M) under vacuum.

The rate constants of BPY compounds were determined by using the following reported equations:<sup>5</sup>

$$\tau_p = 1/k_p \quad \text{Eq-S1}$$

$$\tau_d = 1/k_d \quad \text{Eq-S2}$$

$$k_{\text{ISC}} = (1 - \Phi_F) \times k_p \quad \text{Eq-S3}$$

$$k_{\text{RISC}} = (k_p k_d / k_{\text{ISC}}) \times (\Phi_{\text{TADF}} / \Phi_F) \quad \text{Eq-S4}$$

$$k_r^S = k_p \Phi_F \quad \text{Eq-S5}$$

$$k_{\text{nr}}^T = k_d - k_{\text{RISC}} \Phi_F \quad \text{Eq-S6}$$

$$\Phi_F = \Phi O_2 \quad \text{Eq-S7}$$

$$\Phi_{\text{TADF}} = \Phi N_2 - \Phi_F \quad \text{Eq-S8}$$

**Table S4.** Summarized transient-PL data and the rate constants of TADF dopants.

Emitters <sup>a)</sup>	$\tau_p$ [ns]	$\tau_d$ [μs]	$\Phi_F$ [%] <sup>b)</sup>	$\Phi_{\text{TADF}}$ [%] <sup>b)</sup>	$k_p$ [ $10^6$ s <sup>-1</sup> ] <sup>c)</sup>	$k_d$ [ $10^5$ s <sup>-1</sup> ] <sup>d)</sup>	$k_{\text{IC}}$ [ $10^6$ s <sup>-1</sup> ] <sup>e)</sup>	$k_{\text{ISC}}$ [ $10^7$ s <sup>-1</sup> ] <sup>f)</sup>	$k_{\text{RISC}}$ [ $10^5$ s <sup>-1</sup> ] <sup>g)</sup>	$k_{\text{nr}}^T$ [ $10^4$ s <sup>-1</sup> ] <sup>h)</sup>
<b>26DAcBPY</b>	33	2.3	20	70	6.06	3.91	0.65	2.36	3.52	32.0
<b>25DAcBPY</b>	31	1.9	22	61	7.10	4.37	1.45	2.37	3.63	35.7
<b>26DPXABPy</b>	27	1.0	18	58	6.67	7.60	2.10	2.83	5.78	65.5

<sup>a)</sup>10% BPY compounds measured in mCBP film (30 nm) at 300 K. <sup>b)</sup>PLQY of the prompt fluorescent ( $\Phi_F$ ) component and the delayed fluorescent ( $\Phi_{\text{TADF}}$ ) component. The rate constants of; <sup>c)</sup>prompt fluorescence ( $k_p$ ), <sup>d)</sup>delayed fluorescence ( $k_d$ ), <sup>e)</sup>internal conversion ( $k_{\text{IC}}$ ), <sup>f)</sup>intersystem crossing ( $k_{\text{ISC}}$ ), <sup>g)</sup>reverse intersystem crossing ( $k_{\text{RISC}}$ ), and non-radiative decay ( $k_{\text{nr}}^T$ ).

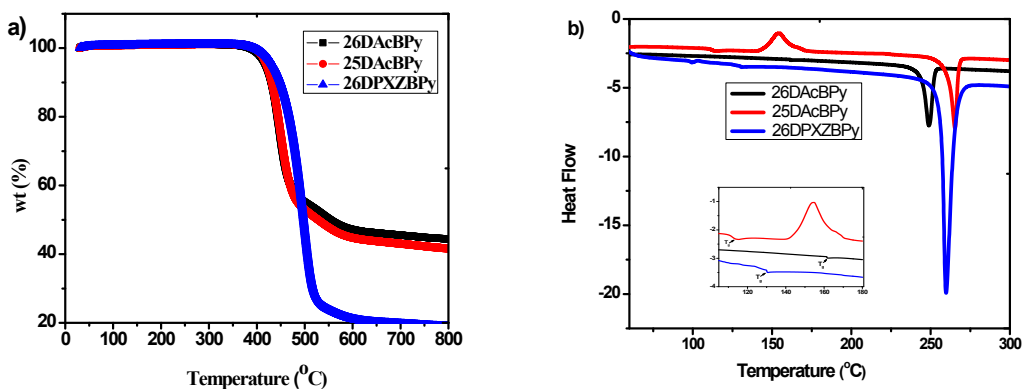


**Fig. S3:** a) TGA curves and b) DSC curves of compounds 26DAcBPY, 25DAcBPY and 26DPXZBPY

### Electrochemical properties and chemical structures of the device materials

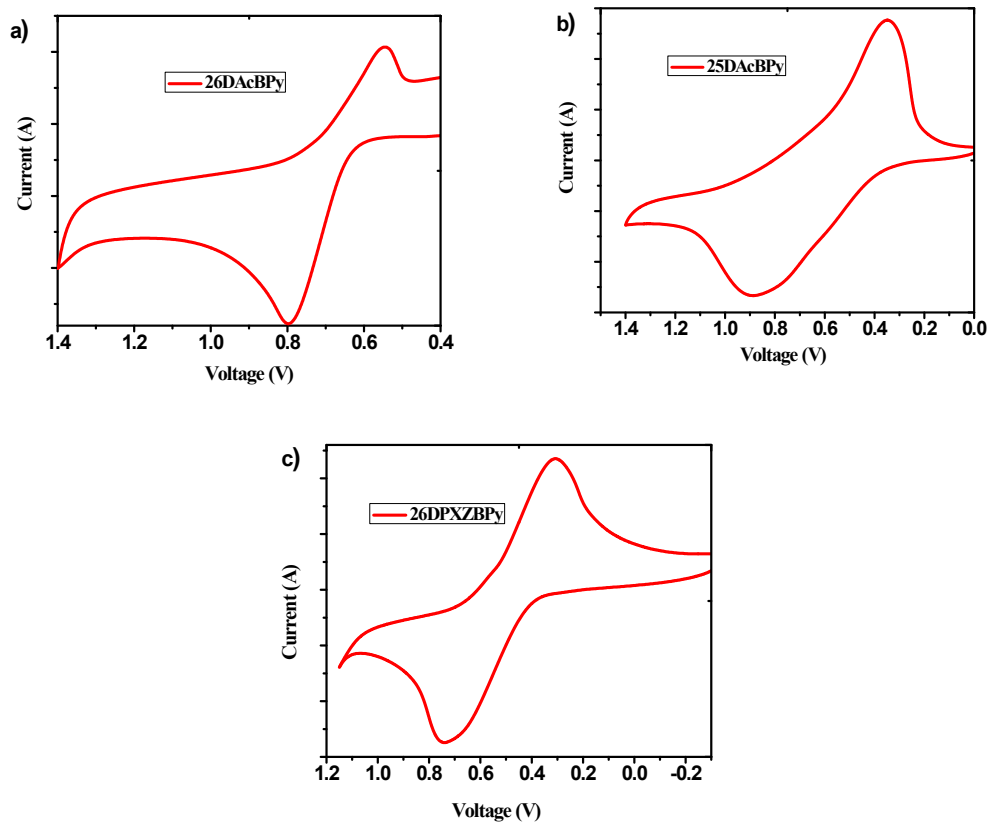


**Fig. S4:** Cyclic voltammogram of compounds a) 26DAcBPY, b) 25DAcBPY, and c) 26DPXZBPY with tetra-butylammonium perchlorate (TBAClO<sub>4</sub>, 0.1 M) was used as a supporting electrolyte in DCM at 10<sup>-3</sup> M solution, and ferrocene (4.8 eV) was used as a reference for calibration.

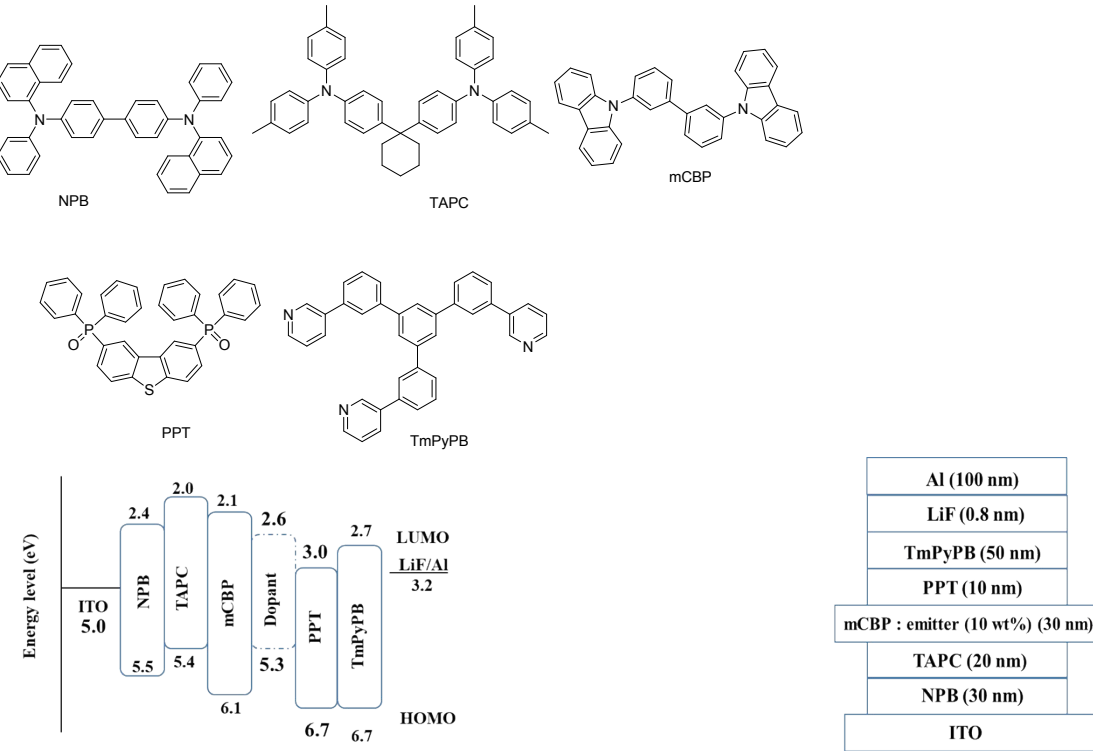


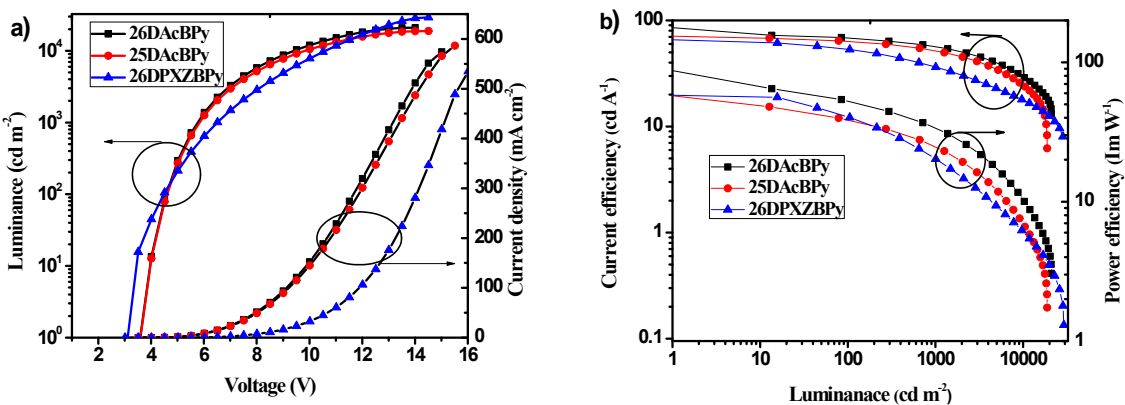
**Fig. S5.** Structures of the materials used in devices and schematic representation of the device

### EL-properties of the devices

Charge balance factor ( $\gamma$ ) calculation:<sup>6</sup>

$$\gamma = \eta_{ext} / \eta_{int} = \eta_{ext} / (\eta_{ST} \times \eta_{out} \times \Phi_F) \quad \text{Eq-S9}$$

where  $\eta_{ext}$  is external quantum efficiency (EQE),  $\eta_{int}$  is internal quantum efficiency (IQE),  $\eta_{ST}$  is the fraction of radiative excitons (100%),  $\eta_{out}$  is the light-out coupling efficiency (ca. 26%) and  $\Phi_F$  is PL quantum yield of the emitting layer



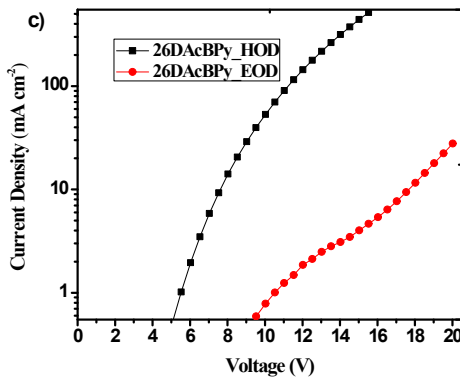


**Fig. S6:** a) Luminance-voltage-current efficiency; b) current efficiency-luminance-power efficiency curves of 26DAcBPY, 25DAcBPY and 26DPXZBPY-based devices; c) the hole and electron only devices with the configurations: ITO/NPB (20 nm)/mCBP: 26DAcBPY (10 wt%) (300 nm)/NPB (50 nm)/Al and ITO/TmPyPB (20 nm)/mCBP: 26DAcBPY (10 wt%) (300 nm)/TmPyPB (50 nm)/ LiF (1 nm)/ Al, respectively.

**Table S5.** EL performances of representative greenish-yellow to yellow-orange TADF OLEDs.<sup>a</sup>

Entry	Yellow Emitters	$L_{\max}$ (cd m <sup>-2</sup> )	EQE <sub>max</sub> (%)	EQE (%) at 1,000/10,000cd m <sup>-2</sup>	CIE (x, y)	EL <sub>max</sub>	Ref
1	26DAcBPY	20334	23.1	17.4/7.8	(0.37, 0.57)	542	This work
2	25DAcBPY	18055	19.6	14.5/6.0	(0.42, 0.53)	558	This work
3	26DPXZBPY	29600	13.7	10.9/5.0	(0.49, 0.49)	590	This work
4	6,7-DCQx-Ca	-	21.5	-	(0.37, 0.57)	541	7a
5	5,8-DCQx-Ca	-	20.1	-	(0.47, 0.51)	569	7a
6	34AcCz-Trz	-	14.2	-	(0.40, 0.56)	540	7b
7	SFDBQPXZ	31790	23.5	13.0/-	-	548	7c
8	DFDBQPXZ	31099	16.8	12.4/-	-	548	7c
9	CP-BP-PXZ	27540	19.1	12.0/-	(0.37, 0.57)	542	7d
10	CP-BP-DMAC	32250	19.6	13.6/-	(0.38, 0.57)	542	7d
11	DPXZ-as-TAZ	10020	9.6	8.0/-	(0.44, 0.52)	-	7e
12	TPXZ-as-TAZ	11270	13.0	11.5/-	(0.44, 0.52)	-	7e
13	PxPmBPX	61040	11.3	-	-	541	7f
14	PXZDS02	17000	16.7	13.7/-	(0.44, 0.54)	549	7g
15	TBP-PXZ	49240	17.7	16.0/12.7	(0.45, 0.53)	564	7h
16	Ac-CNP	70630	13.3	9.1/6	(0.47, 0.51)	580	3
17	MoCz-PCN	43785	20.6	16.6/-	(0.38, 0.57)	-	8a
18	4CzCNPy	-	6.6	-	(0.37, 0.59)	536	8b

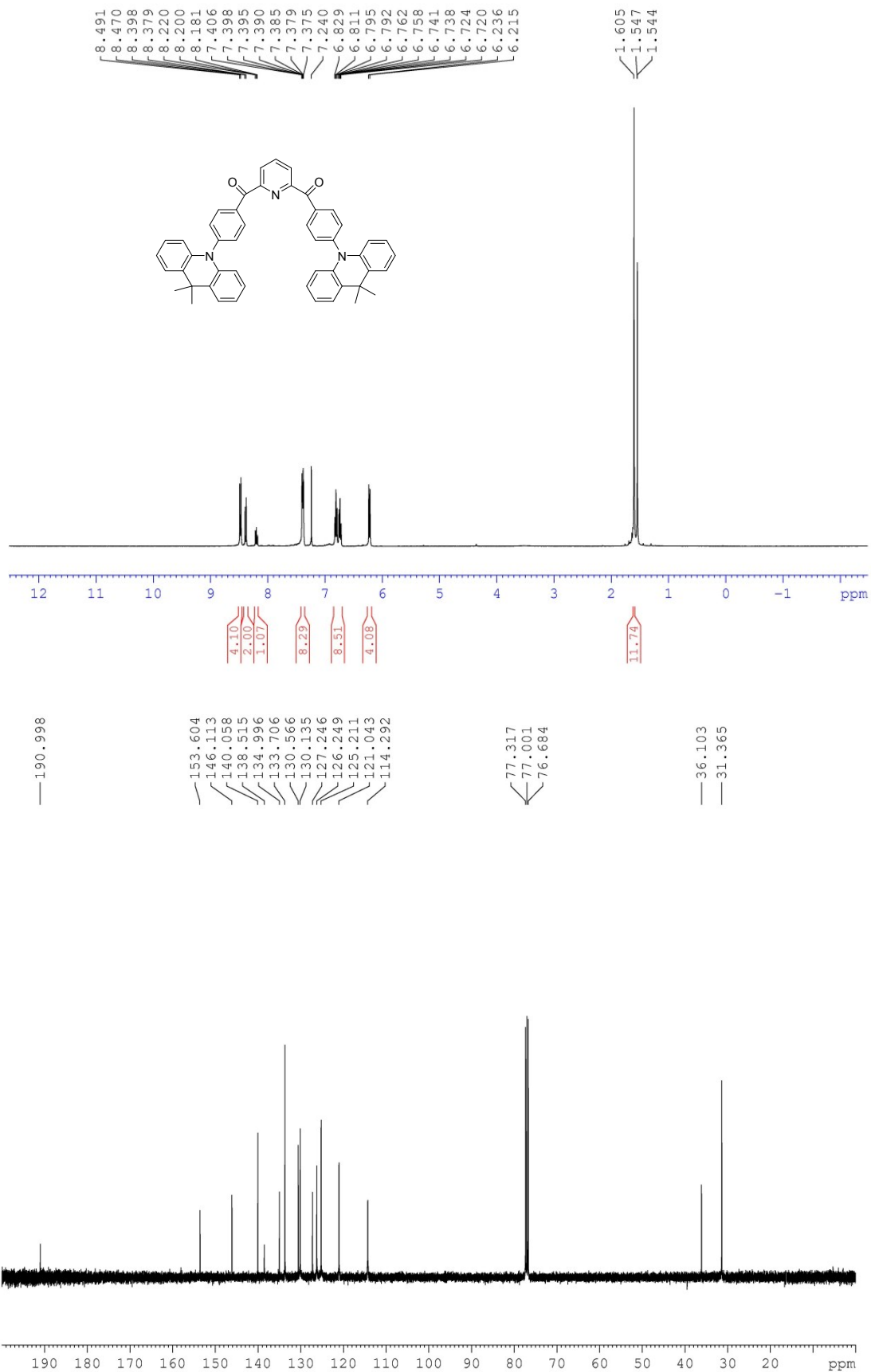
19	Py56	-	29.2	20.6/-	(0.43,0.55)	-	8c
20	CzPyCN	6034	7.4	-	(0.38,0.53)	536	8d

<sup>a</sup> The results were obtained from reference.

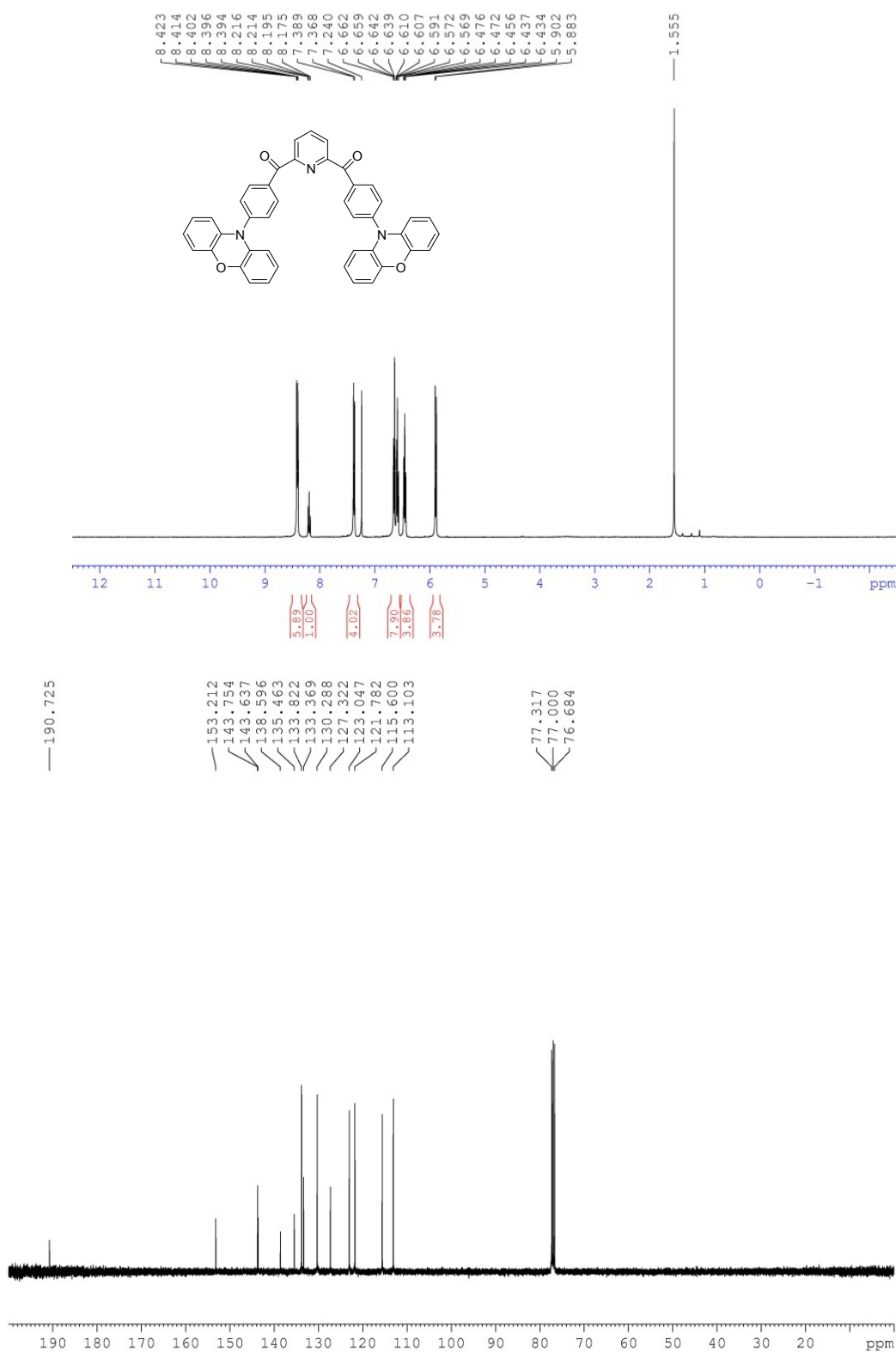
## References

- 1 C. Adamo and V. Barone, *J. Chem. Phys.*, 1999, **110**, 6158-6170.
- 2 M. Ernzerhof and G. E. Scuseria, *J. Chem. Phys.*, 1999, **110**, 5029-5036.
- 3 I. S. Park, S. Y. Lee, C. Adachi and T. Yasuda, *Adv. Funct. Mater.*, 2016, **26**, 1813-1821.
- 4 W. Ryan, A. Jennifer, E. Oleg, H. F. Tsao, H. Zihao, H. J. Brooks, L. Patricia, O. Philip, R. Karina, S. Laurie, S. John, T. Nuria and Z. X. Mei, US patent, US2014/213581, 2014.
- 5 S. Kothavale, K. H. Lee and J. Y. Lee, *ACS Appl. Mater. Interfaces*, 2019, **11**, 17583-17591.
- 6 S. Gan, S. Hu, X.-L. Li, J. Zeng, D. Zhang, T. Huang, W. Luo, Z. Zhao, L. Duan, S.-J. Su and B. Z. Tang, *ACS Appl Mater Interfaces*, 2018, **10**, 17327-17334.
- 7 Triazine- and carbonyl-based TADF materials see: (a) S. Kothavale, K. H. Lee and J. Y. Lee, *ACS Appl. Mater. Interfaces*, 2019, **11**, 17583-17591; (b) Q. Zhang, S. Sun, W. Liu, P. Leng, X. Lv, Y. Wang, H. Chen, S. Ye, S. Zhuang and L. Wang, *J. Mater. Chem. C*, 2019, DOI: 10.1039/C9TC01329F; (c) L. Yu, Z. Wu, G. Xie, C. Zhong, Z. Zhu, D. Ma and C. Yang, *Chem. Commun.*, 2018, **54**, 1379-1382; (d) J. Huang, H. Nie, J. Zeng, Z. Zhuang, S. Gan, Y. Cai, J. Guo, S.-J. Su, Z. Zhao and B. Z. Tang, *Angew. Chem. Int. Ed.*, 2017, **56**, 12971-12976; (e) Y. Xiang, S. Gong, Y. Zhao, X. Yin, J. Luo, K. Wu, Z.-H. Lu and C. Yang, *J. Mater. Chem. C*, 2016, **4**, 9998-10004; (f) S. Y. Lee, T. Yasuda, I. S. Park and C. Adachi, *Dalton Trans.*, 2015, **44**, 8356-8359; (g) G. Xie, X. Li, D. Chen, Z. Wang, X. Cai, D. Chen, Y. Li, K. Liu, Y. Cao and S.-J. Su, *Adv. Mater.*, 2016, **28**, 181-187; (h) Bai, M.-D.; Zhang, M.; Wang, K.; Shi, Y.-Z.; Chen, J.-X.; Lin, H.; Tao, S.-L.; Zheng, C.-J.; Zhang, X.-H. M.-D. Bai, M. Zhang, K. Wang, Y.-Z. Shi, J.-X. Chen, H. Lin, S.-L. Tao, C.-J. Zheng and X.-H. Zhang, *Org. Electron.*, 2018, **62**, 220-226.
- 8 Pyridine-based TADF materials see: (a) Z. Chen, F. Ni, Z. Wu, Y. Hou, C. Zhong, M. Huang, G. Xie, D. Ma and C. Yang, *J. Phys. Chem. Lett.*, 2019, **10**, 2669-2675; (b) X. Cao, X. Zhang, C. Duan, H. Xu, W. Yuan, Y. Tao and W. Huang, *Org. Electron.*, 2018, **57**, 247-254; (c) K. C. Pan, S. W. Li, Y. Y. Ho, Y. J. Shiu, W. L. Tsai, M. Jiao, W. K. Lee, C. C. Wu, C. L. Chung, T. Chatterjee, Y. S. Li, K. T. Wong, H. C. Hu, C. C. Chen and M. T. Lee, *Adv. Funct. Mater.*, 2016, **26**, 7560-7571; (d) Q. Wu, M. Wang, X. Cao, D. Zhang, N. Sun, S. Wan and Y. Tao, *J. Mater. Chem. C*, 2018, **6**, 8784-8792.

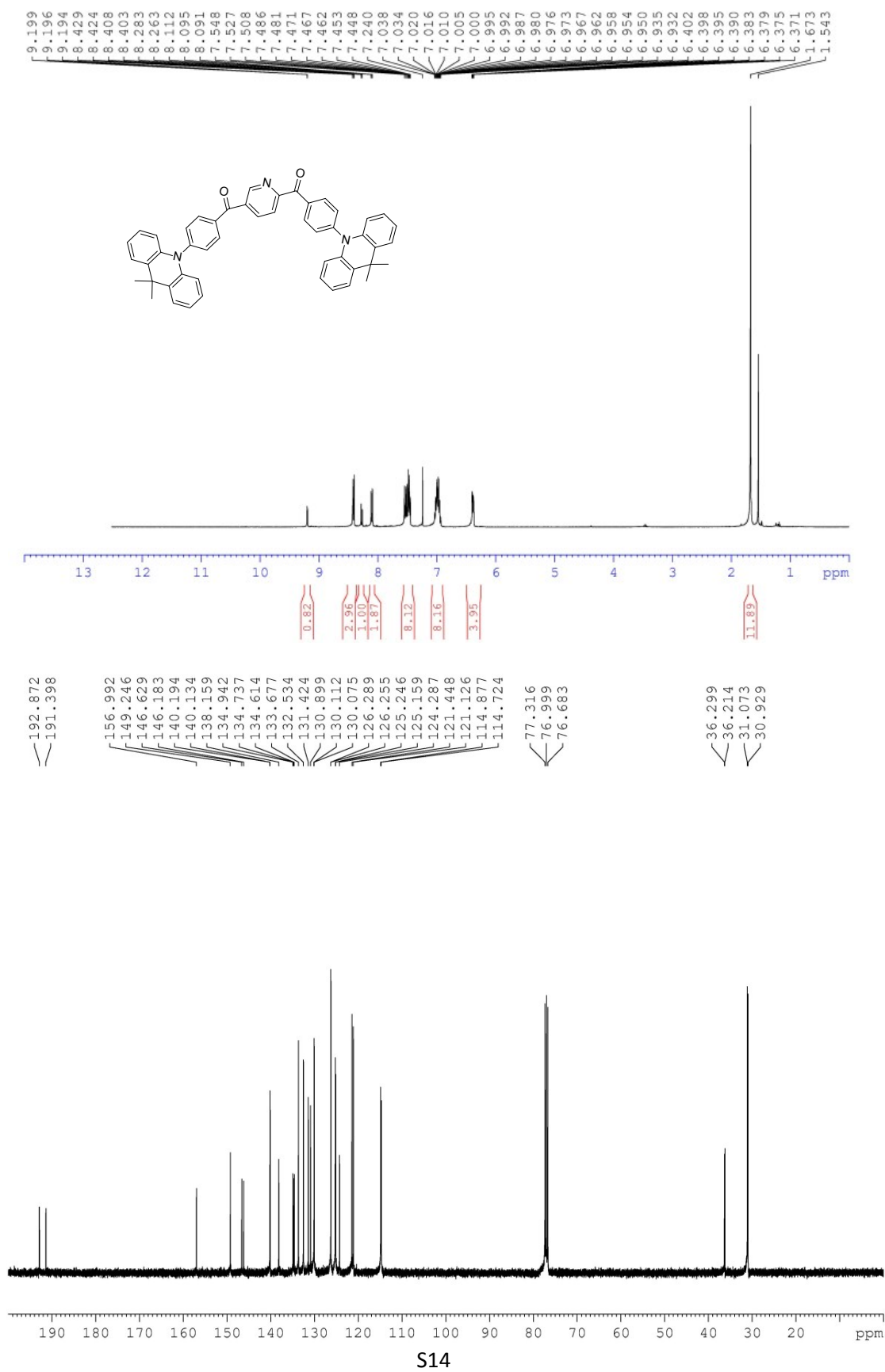
## **<sup>1</sup>H & <sup>13</sup>C NMR spectra of compound 26DAcBPy**



## <sup>1</sup>H & <sup>13</sup>C NMR spectra of compound 26DPXZBPy



### **<sup>1</sup>H & <sup>13</sup>C NMR spectra of compound 25DAcBPy**



### X-Ray crystallographic analysis:

**General Crystal Growing Conditions:** X-ray quality single crystals of **26DAcBPY**, **25DAcBPY** and **26PXZBPY**, were collected from the sublimed tube after cooling down to room temperature (sublimed temperatures are 260, 275, and 290 °C for **26DAcBPY**, **25DAcBPY** and **26PXZBPY**, respectively).

ORTEP diagram of compound **26DAcBPY** (CCDC = 1906824)

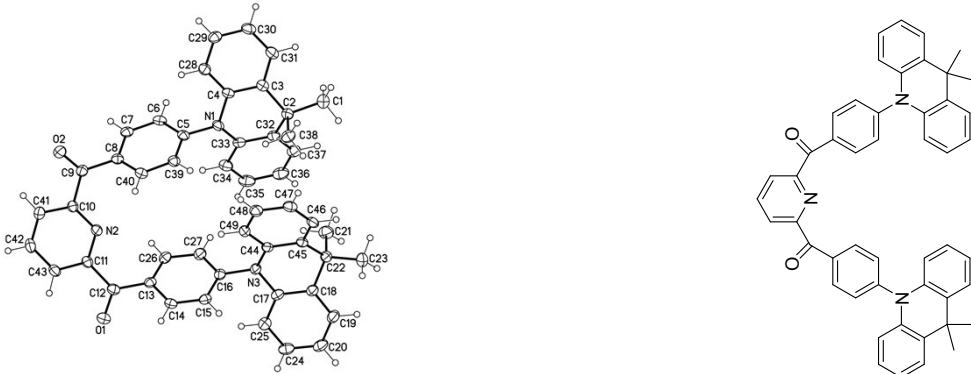


Table S6. Crystal data and structure refinement for 180220LT\_0M.

Identification code	180220LT_0m	
Empirical formula	C <sub>49</sub> H <sub>39</sub> N <sub>3</sub> O <sub>2</sub>	
Formula weight	701.83	
Temperature	100(2) K	
Wavelength	0.71073 Å	
Crystal system	Triclinic	
Space group	P -1	
Unit cell dimensions	a = 10.3324(4) Å	α = 77.029(2)°.
	b = 14.3340(5) Å	β = 80.766(2)°.
	c = 26.1832(10) Å	γ = 74.062(2)°.
Volume	3613.4(2) Å <sup>3</sup>	
Z	4	
Density (calculated)	1.290 Mg/m <sup>3</sup>	
Absorption coefficient	0.079 mm <sup>-1</sup>	
F(000)	1480	
Crystal size	0.20 x 0.15 x 0.15 mm <sup>3</sup>	
Theta range for data collection	0.802 to 26.365°.	
Index ranges	-12<=h<=12, -17<=k<=17, -32<=l<=32	
Reflections collected	57089	
Independent reflections	14633 [R(int) = 0.0366]	
Completeness to theta = 25.242°	99.7 %	

Absorption correction	Semi-empirical from equivalents
Max. and min. transmission	0.9485 and 0.9015
Refinement method	Full-matrix least-squares on $F^2$
Data / restraints / parameters	14633 / 0 / 981
Goodness-of-fit on $F^2$	1.029
Final R indices [ $I > 2\sigma(I)$ ]	$R_1 = 0.0493$ , $wR_2 = 0.1009$
R indices (all data)	$R_1 = 0.0772$ , $wR_2 = 0.1181$
Extinction coefficient	n/a
Largest diff. peak and hole	0.250 and -0.234 e. $\text{\AA}^{-3}$

ORTEP diagram of compound **25DAcBPy** (CCDC = 1906825)

### 1) Without H-bonding conformation about 34%

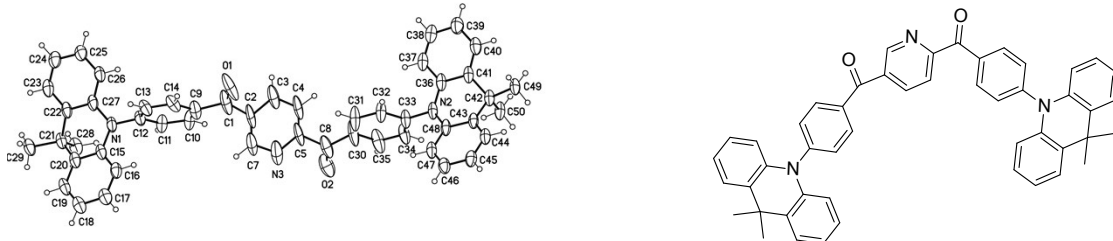


Table S7a. Crystal data and structure refinement for 170750lt3\_0m\_a.

Identification code	170750lt3_0m_a		
Empirical formula	C49 H39 N3 O2		
Formula weight	701.83		
Temperature	100(2) K		
Wavelength	0.71073 $\text{\AA}$		
Crystal system	Triclinic		
Space group	P -1		
Unit cell dimensions	$a = 9.1080(5) \text{ \AA}$	$\alpha = 97.767(2)^\circ$	
	$b = 9.7627(5) \text{ \AA}$	$\beta = 97.520(2)^\circ$	
	$c = 20.9805(10) \text{ \AA}$	$\gamma = 98.633(2)^\circ$	
Volume	$1805.61(16) \text{ \AA}^3$		
Z	2		
Density (calculated)	1.291 Mg/m <sup>3</sup>		

Absorption coefficient	0.079 mm <sup>-1</sup>
F(000)	740
Crystal size	0.16 x 0.13 x 0.05 mm <sup>3</sup>
Theta range for data collection	0.991 to 26.402°.
Index ranges	-7<=h<=11, -12<=k<=11, -25<=l<=26
Reflections collected	25617
Independent reflections	7361 [R(int) = 0.0365]
Completeness to theta = 25.242°	99.8 %
Absorption correction	Semi-empirical from equivalents
Max. and min. transmission	0.9485 and 0.8873
Refinement method	Full-matrix least-squares on F <sup>2</sup>
Data / restraints / parameters	7361 / 372 / 583
Goodness-of-fit on F <sup>2</sup>	1.058
Final R indices [I>2sigma(I)]	R1 = 0.1040, wR2 = 0.2691
R indices (all data)	R1 = 0.1382, wR2 = 0.2978
Extinction coefficient	0.009(2)
Largest diff. peak and hole	0.977 and -0.679 e.Å <sup>-3</sup>

## 2 With H-bonding conformation about 66%

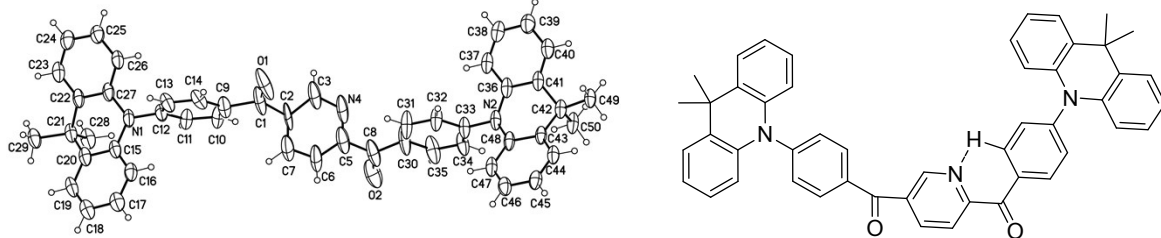


Table S7b. Crystal data and structure refinement for 170750lt3\_0m\_a.

Identification code	170750lt3_0m_a
Empirical formula	C49 H39 N3 O2
Formula weight	701.83
Temperature	100(2) K
Wavelength	0.71073 Å
Crystal system	Triclinic
Space group	P-1
Unit cell dimensions	a = 9.1080(5) Å      α = 97.767(2)°.

	$b = 9.7627(5) \text{ \AA}$	$\beta = 97.520(2)^\circ$
	$c = 20.9805(10) \text{ \AA}$	$\gamma = 98.633(2)^\circ$
Volume	$1805.61(16) \text{ \AA}^3$	
Z	2	
Density (calculated)	$1.291 \text{ Mg/m}^3$	
Absorption coefficient	$0.079 \text{ mm}^{-1}$	
F(000)	740	
Crystal size	$0.16 \times 0.13 \times 0.05 \text{ mm}^3$	
Theta range for data collection	1.983 to 26.402°.	
Index ranges	$-7 \leq h \leq 11, -12 \leq k \leq 11, -25 \leq l \leq 26$	
Reflections collected	25607	
Independent reflections	7360 [ $R(\text{int}) = 0.0365$ ]	
Completeness to theta = 25.242°	99.8 %	
Absorption correction	Semi-empirical from equivalents	
Max. and min. transmission	0.9485 and 0.8873	
Refinement method	Full-matrix least-squares on $F^2$	
Data / restraints / parameters	7360 / 366 / 571	
Goodness-of-fit on $F^2$	1.055	
Final R indices [ $I > 2\sigma(I)$ ]	$R_1 = 0.1039, wR_2 = 0.2587$	
R indices (all data)	$R_1 = 0.1379, wR_2 = 0.2831$	
Extinction coefficient	0.0047(18)	
Largest diff. peak and hole	0.959 and -0.605 e. $\text{\AA}^{-3}$	

### ORTEP diagram of compound **26DPXZBPy** (CCDC = 1906826)

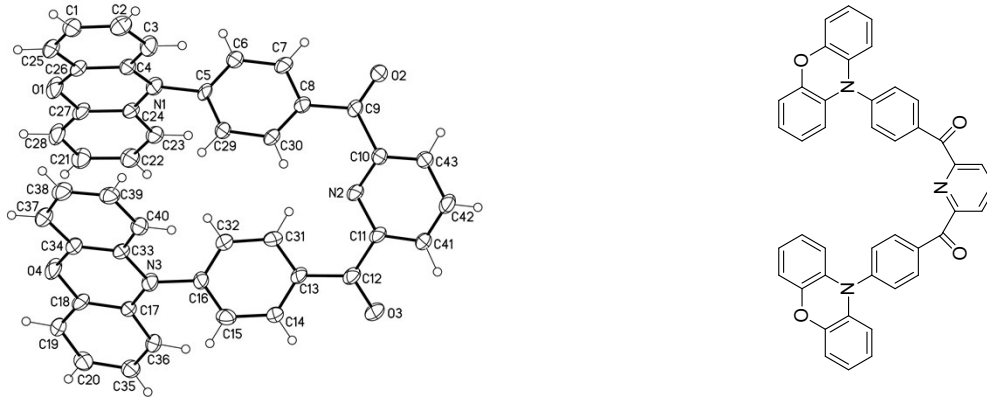


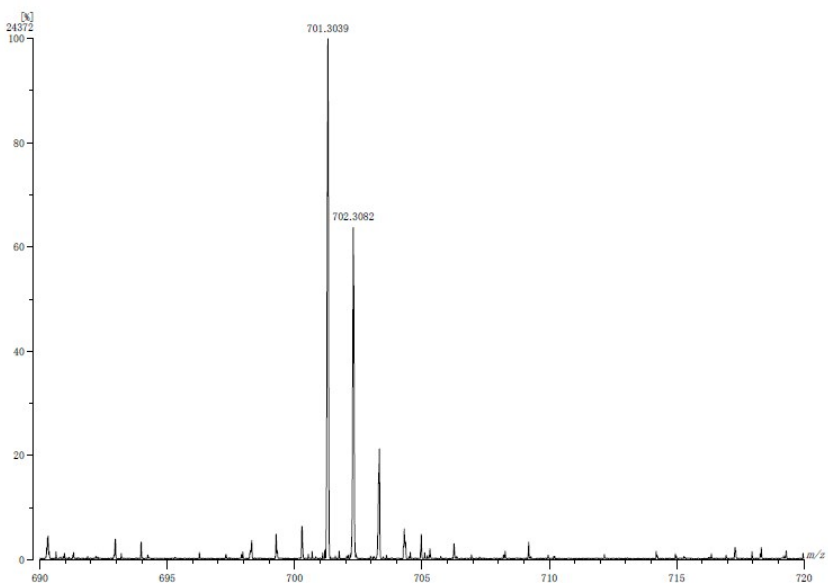
Table S8. Crystal data and structure refinement for mo\_170906lt\_0m.

Identification code	mo_170906lt_0m		
Empirical formula	C43 H27 N3 O4		
Formula weight	649.67		
Temperature	100(2) K		
Wavelength	0.71073 Å		
Crystal system	Triclinic		
Space group	P -1		
Unit cell dimensions	a = 11.35(2) Å	α= 111.73(4)°.	
	b = 11.79(2) Å	β= 94.96(5)°.	
	c = 12.45(2) Å	γ = 92.64(4)°.	
Volume	1537(5) Å <sup>3</sup>		
Z	2		
Density (calculated)	1.404 Mg/m <sup>3</sup>		
Absorption coefficient	0.091 mm <sup>-1</sup>		
F(000)	676		
Crystal size	0.22 x 0.15 x 0.04 mm <sup>3</sup>		
Theta range for data collection	1.772 to 26.595°.		
Index ranges	-13<=h<=14, -14<=k<=13, -10<=l<=15		
Reflections collected	21434		
Independent reflections	6215 [R(int) = 0.1177]		
Completeness to theta = 25.242°	99.9 %		
Absorption correction	Semi-empirical from equivalents		
Max. and min. transmission	0.9485 and 0.5056		
Refinement method	Full-matrix least-squares on F <sup>2</sup>		
Data / restraints / parameters	6215 / 0 / 451		
Goodness-of-fit on F <sup>2</sup>	0.969		
Final R indices [I>2sigma(I)]	R1 = 0.0805, wR2 = 0.1931		
R indices (all data)	R1 = 0.1382, wR2 = 0.2285		
Extinction coefficient	n/a		
Largest diff. peak and hole	0.443 and -0.469 e.Å <sup>-3</sup>		

## Mass spectral analysis of TADF emitters:

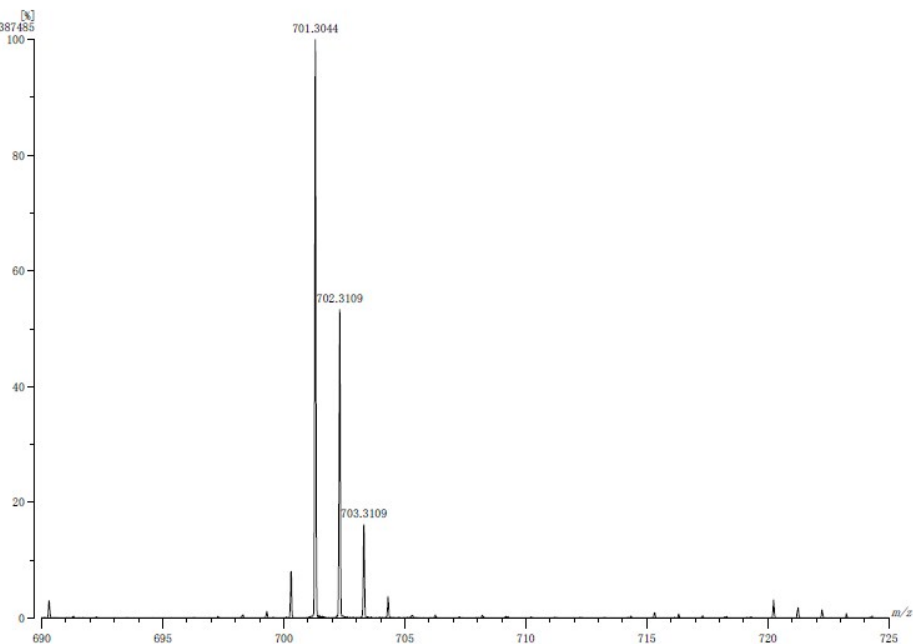
### a) 26DAcBPY

[ Mass Spectrum ]  
 Data : 1015 Date : 02-Feb-2018 15:35  
 Instrument : MSstation  
 Sample : P1  
 Notes:  
 Inlet : Direct Ion Mode : EI+  
 Spectrum Type : Normal Ion [EF=Linear]  
 RT : 3.52 min Scan# : 146 Temp : 3276.7 deg.C  
 BP : m/z 701.3039 Int. : 2.32 (24372)  
 Output m/z range : 690 to 720 Cut Level : 0.00 %



### b) 25DAcBPY

[ Mass Spectrum ]  
 Data : 1016 Date : 02-Feb-2018 15:53  
 Instrument : MSstation  
 Sample : P2  
 Notes:  
 Inlet : Direct Ion Mode : EI+  
 Spectrum Type : Normal Ion [EF=Linear]  
 RT : 1.65 min Scan# : 69 Temp : 3276.7 deg.C  
 BP : m/z 701.3044 Int. : 36.95 (387485)  
 Output m/z range : 690 to 725 Cut Level : 0.00 %



c) 26DPXZBPY

